Int. J. Electrochem. Sci., 17 **(2022)** Article Number: 220712, doi: 10.20964/2022.07.07

International Journal of
ELECTROCHEMICAL
SCIENCE
www.electrochemsci.org

Detection of Esophageal Cancer Marker CA19-9 Based on MXene Electrochemical Immunosensor

Qifei Wang[1], *Fei Chen*[2], *Lingdong Qiu*[1], *Yushu Mu*[1], *Shibin Sun*[1], *Xulong Yuan*[1], *Pan Shang*[1], *Bo Ji*[*]

[1] Department of Cerebral Surgery, The Second Affiliated Hospital of Shandong First Medical University, Taian, 271000, China
[2] Digestive System Department, The Second Affiliated Hospital of Shandong First Medical University, Taian, 271000, China
[*]E-mail: jibo_tsahotfmu@163.com

Received: 5 February 2022 / *Accepted:* 18 March 2022 / *Published:* 6 June 2022

Carbohydrate antigen-19-9 (CA19-9) is an abnormal tumor marker in the blood of many patients with esophageal cancer, thus a rapid test for CA19-9 is conducive to the diagnosis of cancer. The end of MXene surface is rich in -OH, -O and F functional groups, which can be used as a modification to construct electrochemical sensors. This work reports on a MXene-based electrochemical sensor for the highly sensitive detection of CA19-9. XPS and XRD were used to characterize the materials. Under optimal conditions, this sensor can quickly detect CA19-9 from 0.002 to 30 U/mL. The detection limit can be as low as 0.001 U/mL. In addition, the sensor was successfully adopted to detect the CA19-9 in the serum.

Keywords: CA19-9, Esophageal cancer, Electrochemical detection, MXene, Immunosensor

1. INTRODUCTION

Esophageal cancer is the eighth most common cancer in the world and the sixth most common cancer in terms of death rates. Esophageal cancer is the fifth leading cancer and the fourth leading cause of cancer death in China. It can be classified as squamous and glandular types, and the squamous type is the most common esophageal cancer in China. Despite that great progress has been made in the treatment technology of esophageal cancer in recent years, the malignant degree of esophageal cancer is still high, the course of disease progresses rapidly, and it is easy to relapse and metastasize [1–5]. A large number of experiments show that the occurrence and development of esophageal cancer is related to multiple genes and factors, and the specific markers for the diagnosis and treatment of esophageal cancer

still need to be further studied. Screening efficient and specific molecular biomarkers for esophageal cancer is of great significance for the diagnosis, treatment and prognosis of esophageal cancer [6–10].

Sampling from local tumor tissue by biopsy or microdissection is difficult and invasive. Therefore, it is recommended to identify biomarkers from body fluids readily available in general clinical practice, such as serum, saliva, urine, brain crest fluid, etc. Serum contains a large number of proteins and molecules [11,12], thus serum circulation provides the most up-to-date information on human proteomics. Proteomics has become a powerful technique for explaining biological processes, representing the large-scale role building of proteins, including complex features such as isomers, modifications, interactions and functional structures [13–15]. Many biomarkers in biopsied cancer tissue can also be found in blood. Since the ultimate goal of detecting biomarkers is to conduct specific, early and non-invasive diagnosis and post-treatment monitoring of cancer, blood is an appropriate biomaterial. In the past few years, several studies have reported serological biomarkers in various combinations. However, currently there are no reliable and validated biomarkers with specificity, sensitivity and stability. Therefore, a multi-biomarker that can improve the accuracy of early diagnosis is urgently needed. Tumor markers can be described as molecular products expressed in tumor tissue or metabolized and secreted by tumor, which have biochemical characteristics in body fluids such as blood and urine [16,17]. They can be adopted as indicators of tumor staging and grading to monitor the response to treatment and predict recurrence, progression, metastasis, and even patient survival. Carbohydrate antigen-19-9 (CA19-9) is an abnormally high tumor marker in the blood of many patients with esophageal cancer. The development of a rapid test for CA19-9 is of great help in the diagnosis of cancer. With the improvement of human living standards, the demand for new materials has also been increasing [18–20]. The excellent chemical and physical properties of two-dimensional materials have received extensive attention from international researchers. MXene is a two-dimensional material of transition metals, similar to the layered structure of graphene. The versatility and adjustable properties of MXene, including excellent electrical conductivity, hydrophilicity and intercalation, make MXene an excellent candidate for a number of applications. These favorable electrochemical properties have allowed this new 2D material to be adopted primarily for energy conversion and storage applications [21–24]. In addition, it is also applied in a wide range of emerging fields in electronics, sensing and photonics.

The advantages of MXene or its composite materials, such as high mechanical flexibility, good ductility and excellent electrical conductivity, attract a large number of researchers to adopt MXene to construct sensors with different functions [25–27]. MXene can be mixed with other materials to improve the sensitivity of sensors. The end of MXene surface is rich in -OH, -O and F functional groups, and other functional groups present negative charges [28–30], thus positively charged molecules can be adsorbed on the surface of MXenes by electrostatic force [30,31]. The composite material has strong sensing ability, excellent mechanical properties, and hydrophilicity, and it is easy to control. In this work, an electrochemical sensor for the detection of CA19-9 was assembled with MXene modified conventional glassy carbon electrode (GCE).

2. MATERIALS AND METHODS

Ti_3AlC_2, 1-ethyl-3-(3-dimethylaminopropyl) carbodiimide (EDC), glutaraldehyde, horseradish peroxidase (HRP), thionine (TH) and N-hydroxysuccinimide (NHS) were purchased from Aiyuan Chemical Co. Ltd. Graphene sheets (GS) were purchased from Pioneer Nanomaterials Inc. The CA19-9, antibody CA19-9 (Ab1) and CA19-9 (Ab2) were purchased from Yeshenghua Biotech Co. Ltd. All of the other reagents were of analytical quality and were utilized without any additional purification or purifying steps. The electrolyte utilized throughout the experiment was phosphate-buffered saline (PBS). Ultrapure water was adopted as a solvent in the following electrochemical studies.

The multilayer $Ti_3C_2T_x$ MXene was synthesized in accordance with the published procedures [32], with only minor alterations. After being incubated for five hours in an HF solution at room temperature with 10 grams of Ti_3AlC_2 powder (stacked MXene), a tip sonicator was used to accomplish sonic delamination on $Ti_3C_2T_x$ for 0.5 h (MXene).

To make the MXene/HRP/Ab2 conjugation, 2 mg of MXene was dispersed into 4 mL of PBS, which was then incubated for 60 minutes with 2 mL of Ab2 solution (5 g/mL) + HRP solution (50 g/mL).

GCE was cleaned and dried in the open air. The GS/TH solution (5 μL) was applied to the surface of this GCE, which was then dried. The CA19-9 antibody (Ab1) was immobilized on the modified GCE. The subsequent addition of EDC/NHS boosted the reaction, after which the electrode was rinsed. After 0.5 hours incubation in BSA solution (1%) to prevent nonspecific binding sites, this electrode was incubated for 60 minutes with CA19-9 solution at various concentrations before being dripped with the MXene/MSN/HRP/Ab2 solution. Afterwards, the electrode was rinsed and incubated for another 60 minutes before being used.

On a CHI760E Electrochemical Analyzer with a three-electrode setup, all electrochemical experiments were conducted. As the working electrode, a glassy carbon electrode (GCE) was utilized. A simple drop casting technique was adopted for the GCE surface modification. The current signal was obtained by the catalytic reaction caused by HRP. The potentiostatic (-0.3V) detection was adopted to record the current signal of different sensors.

3. RESULTS AND DISCUSSION

Before and after the delamination of MXene, the layered structure of MXene is visible after HF etching with the layers separated [33]. Thinner MXene multi-layer films were observed after delamination. The $Ti_3C_2T_x$ sheets have high aqueous solution dispersibility and may be employed for the direct modification of GCE surface [34].

XRD (Figure 1A) and XPS (Figure 1B) were adopted to assess the quality of the MXene that had been synthesized. The XRD pattern reveals the MXene (002) peak, which moves from 9.48 degrees in MXene, indicating that the etching procedure increased the d-spacing between layers. Signals from Ti, C, O, and F elements may be seen in the XPS scan. The presence of F and O means that the MXene surface was terminated by -F and -O groups [35].

The interface property was analyzed with electrochemical impedance spectroscopy. As illustrated in Figure 2, both GCE and MXene/GCE exhibit a semicircle portion in the high frequency

range, which is consistent with an electron transfer-limited process. GCE and MXene/GCE have charge transfer resistances of 871 and 598 Ω, respectively, which implies that modifying the commercial electrode surface with MXene might marginally increase its electrochemical performance owing to its superior conductivity and large surface area. Despite the outstanding electrical characteristics, the negative dipole and hydrophobicity of the surface, which are related with the fluorine termination, may hinder electron transfer kinetics. These findings can be explained by the shape of the MXene employed to modify the electrode surface.

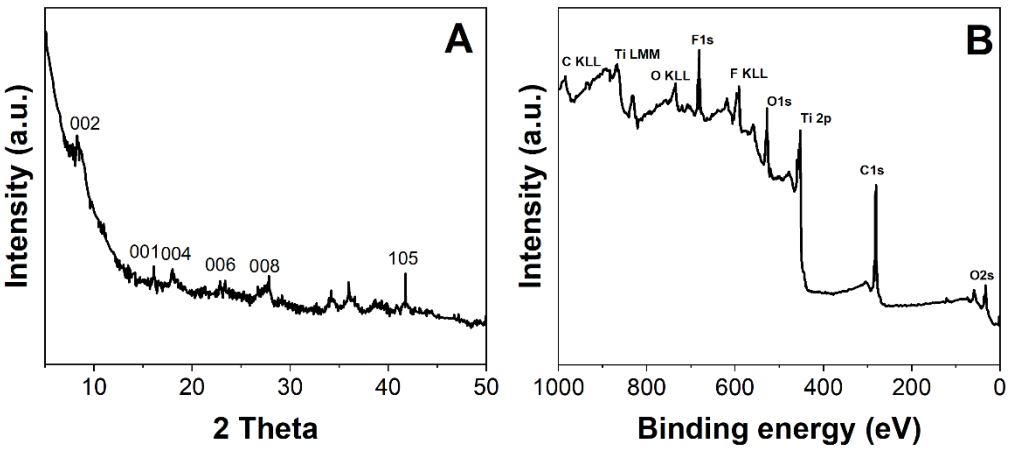

Figure 1. (A) XRD pattern and (B) XPS survey of MXene.

A modified GCE was created in this work by surface casting a MXene dispersion (dubbed MXene(stacked)/GCE). As seen in Figure 2, the charge transfer resistance of the MXene(stacked)/GCE is 1904 Ω, which is much more than the charge transfer resistance of bare GCE. A well-delaminated MXene dispersion can form a flat and continuous thin film on the electrode surface, allowing the full access to the electrode's electronic superiority while minimising surface fluorine termination effects [36].

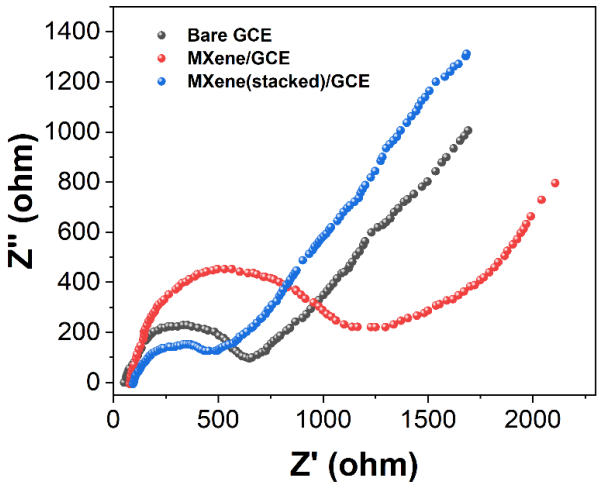

Figure 2. Electrochemical impedance spectroscopy of bare GCE, MXene/GCE and MXene(stacked)/GCE in 5 mM $Fe(CN)_6^{3-/4-}$ and 0.1 M KCl.

According to a recent work, the MXene might be employed directly for electrochemical sensing applications in the cathodic potential window due to the possibility of MXene oxidation at potentials greater than 180 mV. However, an anodic cyclic voltammetry (CV) scan of the MXene/GCE shows no detectable oxidation peak, indicating that the $Ti_3C_2T_x$ is stable during the scan range studied [37]. This result can be explained by the varied surface chemical states of MXene as a consequence of the preparation procedure. In this work, the MXene/GCE was used for anodic potential sensing. Meanwhile, MXene's two-dimensional structure makes the interface of electrochemical sensor composed by it has the advantage of being relatively stable and will not fall off directly in the process of detection [38,39].

The comparison of various electrodes was shown in Figure 3, which is to determine the advantages of our suggested immunoassay, where a large current was detected on the MXene/HRP/Ab2/GCE. Since the current signal is obtained by the catalytic reaction caused by HRP, the potentiostatic (-0.3V) detection was adopted to record the current signal of different sensors. MXene/HRP/Ab2/GCE and HRP/Ab2/GCE were also utilized as probes to determine the influence of MXene/HRP on the measurement's sensitivity. Initially, the same batch of sensors were employed with the same concentration of CA19-9. Subsequently, two more probes were used. In comparison to the signal obtained with HRP/anti-CA19-9, the MXene/HRP/Ab2/GCE showed a more significant response due to the enhancement of thionine and Ab2 immobilization density. The electron transfer rate can be enhanced with thionine being used as a mediator, where a high number of HRP can be attracted on the electrode surface [40,41]. The transported HRP molecules demonstrated a much greater catalytic effectiveness than the thionine-H_2O_2 system or the reaction employing simply the HRP-labeled Ab2. It can be ascribed to the large protein immobilized on the electrode which prevents electron transport from the solution to the electrode's surface [42]. As a result, the MXene loaded HRP can increase the sensing performance towards CA19-9.

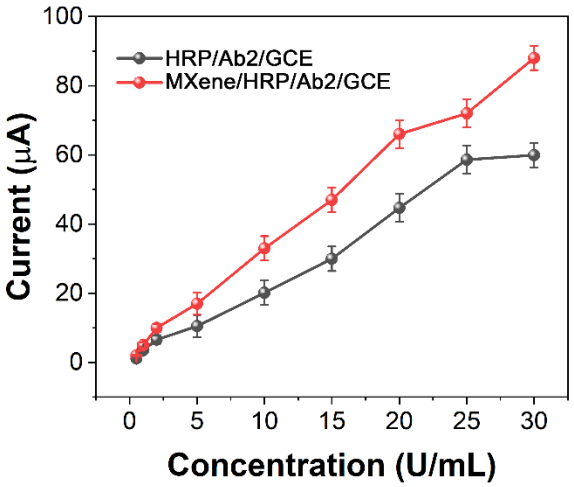

Figure 3. Currents of the sensor towards different concentrations of CA19-9: MXene/HRP/Ab2/GCE and HRP/Ab2/GCE in PBS + 5.0 mM H_2O_2.

The first signal amplification was caused by the increase in the amount of HRP. It is clear that increasing the quantity of HRP encapsulated in the MXene can result in an increase in the electrochemical immunosensor's sensitivity. As a result, HRP at concentrations ranging from 10 to 200 g/mL was employed to optimize HRP encapsulation inside MXene. The CA 19-9 concentration was evaluated electrochemically utilizing a variety of anti-CA19-9 antibody-coated MXene encapsulated with HRP (varied concentrations) [43]. The stripping peak decreased significantly when HRP concentrations increased from 10 to 200 g/mL. There was no discernible reduction in HRP concentrations greater than 200 g/mL. The substantial signal amplification of the MXene/HRP/Ab2 modified GCE bioconjugate may be a result of the synergistic effect of MXene and HRP, which may significantly amplify the electrochemical signal [44–46]. As a result, 200 g/mL was chosen as the optimal HRP concentration for further investigations involving the synthesis of liposomes.

The pH condition of the sensing with MXene/HRP/Ab2/GCE has been optimized for enhancing the sensitivity. Figure 4 illustrates the influence of pH on the detection of CA 19-9 (10 U/mL). After 0.5 hours of incubation at room temperature with the incubation solution + CA19-9 (5 μL, 10 U/mL) and MXene/HRP/Ab (5 μL), our suggested immunosensor was measured with voltammetry in PBS buffer containing 5.0 mM H_2O_2 at a range of pH values. The immunosensor's current shows the presence of an effect. From the test findings, it can be seen that as the PBS pH climbs, the current surges first and subsequently declines, which is consistent with previous reports [47–49]. Nonetheless, since the current response is optimal at pH 7.5, pH 7.5 was chosen as the optimal pH for the CA19-9 measurement.

In addition, the electrochemical sensor can be influenced by the temperature and incubation time. Nonetheless, all experiments were conducted at room temperature to account for their eventual applicability in actual samples. CA19-9 (10 U/mL) was chosen as the sample by varying the length of incubation at room temperature. With the increase of incubation time, a rise in cathodic currents was noted, which tended to diminish after 0.5 h. As a result, 0.5 hours was chosen for the antibody-antigen interaction.

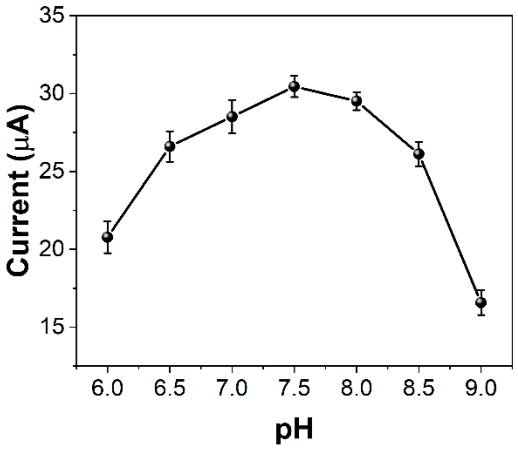

Figure 4. The influence of pH on the detection of CA19-9 (10 U/mL) in the presence of 5.0 mM H_2O_2 using MXene/HRP/Ab2/GCE.

Figure 5 A shows the MXene/HRP/Ab2/GCE towards different concentrations of CA19-9. As the concentration of CA19-9 in the incubation solution grows under ideal circumstances, DPV curves slowly becomes flat. No shift is shown in the response potential, indicating the good repeatability of the sensor. Figure 5B presents a good linear plot between the peak current and the concentrations of CA19-9 from 0.002 to 30 U/mL (R=0.995). The limit of detection (LOD) can be calculated to be 0.001 U/mL (S/N). The narrow error bars indicate that the signal responses are precise. The RSD is within the acceptable range of 4.4-7.2%, indicating that the sensor shows an excellent reproducibility. Table 1 shows the proposed sensor with other previous reported sensors. The comparison reveals that the as-prepared biosensor has a much lower LOD. The encapsulated HRP acquired by amplification acts as a label and significantly increases the sensitivity and linear range. As mentioned above, the as-prepared sensor exhibits the optimal linear range and LOD, and hence has the potential to be utilized to the detection of CA19-9. The intra- and inter-assays were used to determine the repeatability of the proposed sensor. The intra- and inter-assay relative standard deviations (RSD) are all less than 3.6%. The experimental findings indicated that the proposed sensor is reproducible.

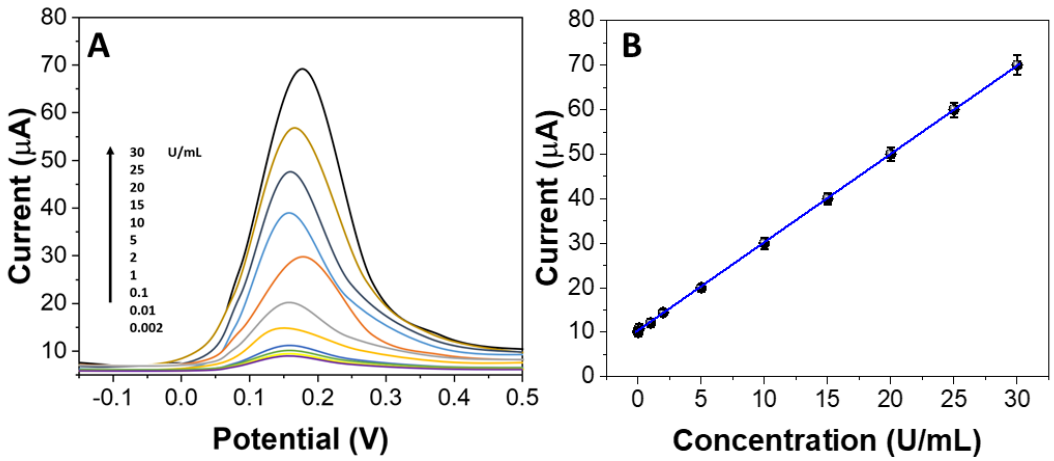

Figure 5. (A) DPV curves of the sensor towards different concentrations of CA 19-9 using MXene/HRP/Ab2/GCE. (B) Corresponding calibration plots.

Table 1 Comparison of the proposed electrochemical sensor with previous reported sensors for CA19-9 detection.

Sensor	LR	LOD	Reference
Polythionine-Au	6.5–520 U/mL	0.26 U/mL	[33]
Polythionine/sodium dodecyl sulphate	5-400 U/mL	0.45 U/mL	[50]
Carbon nanoonions/grphene oxide	0.3-100 U/mL	0.03 U/mL	[28]
Carbon black/polyelectrolytes	0.01-40 U/mL	0.07 U/mL	[51]
MXene/HRP/Ab2/GCE	0.002-30 U/mL	0.001 U/mL	This work

This study makes comparison between the findings of CA19-9 measurement in serum specimens acquired with devised approach and the reference values obtained with a commercially available electrochemiluminescent analyzer. Recovery tests were conducted by introducing CA19-9 at varying concentrations to serum specimens. As shown in Table 2, relative errors for the determination of CA19-9 are less than 3.22%, with a recovery range of 99.04% to 104.02%. These satisfactory findings demonstrate that the specimen determination procedure we created is accurate. The results obtained from the other two procedures corroborate the aforementioned findings. Therefore, our created immunosensor can be employed to detect CA 19-9 in the early stages of diagnosis.

Table 2. Detection of CA19-9 in serum samples using proposed sensor and electrochemiluminescent analyzer.

Sample	Found (U/mL)	Electrochemiluminescent analyzer (U/mL)	RSD (%)	Recovery (%)	Reference (U/mL)
Serum 1	4.51	4.50	1.54	103.04	4.46
Serum 2	22.04	22.03	3.22	99.04	22.38
Serum 3	7.79	7.84	3.13	104.02	7.86

4. CONCLUSION

This work proposes the development of a novel electrochemical sensor for the detection of CA19-9, applying GS/TH as the substrate material, and HRP and MXene as the labels. MXene is a good carrier for secondary antibody and HRP immobilization due to its biocompatibility and wide specific surface area. Its catalytic activity toward H_2O_2 allows the MXene to facilitate the signal response. Compared with the approaches using bare electrodes, this methodology has the potential to increase the signal and sensitivity of our created sensor.

References

1. W. Jin, R. Zhang, C. Dong, T. Jiang, Y. Tian, Q. Yang, W. Yi, J. Hou, *Int. J. Biol. Macromol.*, 144 (2020) 995.
2. N. Feng, Y. Liu, X. Dai, Y. Wang, Q. Guo, Q. Li, *RSC Adv.*, 12 (2022) 1486.
3. A. Thapa, A.C. Soares, J.C. Soares, I.T. Awan, D. Volpati, M.E. Melendez, J.H.T.G. Fregnani, A.L. Carvalho, O.N. Oliveira Jr, *ACS Appl. Mater. Interfaces*, 9 (2017) 25878.
4. J. Li, S. Zhang, L. Zhang, Y. Zhang, H. Zhang, C. Zhang, X. Xuan, M. Wang, J. Zhang, Y. Yuan, *Front. Chem.*, 9 (2021) 339.
5. H. Karimi-Maleh, Y. Orooji, F. Karimi, M. Alizadeh, M. Baghayeri, J. Rouhi, S. Tajik, H. Beitollahi, S. Agarwal, V.K. Gupta, *Biosens. Bioelectron.* (2021) 113252.
6. C.-W. Su, J.-H. Tian, J.-J. Ye, H.-W. Chang, Y.-C. Tsai, *Nanomaterials*, 11 (2021) 1475.
7. C.-W. Su, J.-H. Tian, J.-J. Ye, H.-W. Chang, Y.-C. Tsai, *Nanomaterials*, 11 (2021) 1475.
8. Y. Lv, Z. Zhou, Y. Shen, Q. Zhou, J. Ji, S. Liu, Y. Zhang, *ACS Sens.*, 3 (2018) 1362.
9. S. Wei, X. Chen, X. Zhang, L. Chen, *Front. Chem.*, 9 (2021) 697.

10. H. Karimi-Maleh, A. Khataee, F. Karimi, M. Baghayeri, L. Fu, J. Rouhi, C. Karaman, O. Karaman, R. Boukherroub, *Chemosphere* (2021) 132928.
11. R.-I. Stefan-van Staden, S.S. Gheorghe, R.-M. Ilie-Mihai, M. Badulescu, *J. Electrochem. Soc.*, 168 (2021) 037515.
12. J. Li, X. Ma, M. Li, Y. Zhang, *Biosens. Bioelectron.*, 99 (2018) 438.
13. W. Zhang, G. Xiao, J. Chen, L. Wang, Q. Hu, J. Wu, W. Zhang, M. Song, J. Qiao, C. Xu, *Anal. Bioanal. Chem.*, 413 (2021) 2407.
14. X. Meng, Y. Xu, N. Zhang, B. Ma, Z. Ma, H. Han, *Sens. Actuators B Chem.*, 338 (2021) 129840.
15. Y. Zhuo, R. Yuan, Y.-Q. Chai, C.-L. Hong, *Analyst*, 135 (2010) 2036.
16. R.-I. Stefan-van Staden, R.-M. Ilie-Mihai, F. Pogacean, S. Pruneanu, *J. Porphyr. Phthalocyanines*, 23 (2019) 1365.
17. H. Karimi-Maleh, F. Karimi, L. Fu, A.L. Sanati, M. Alizadeh, C. Karaman, Y. Orooji, *J. Hazard. Mater.*, 423 (2022) 127058.
18. S.L. Oo, S. Venkatesh, V. Karthikeyan, C.M. Arava, S. Pathikonda, P.K. Yu, T.C. Lau, X. Chen, V.A. Roy, *Sensors*, 21 (2021) 2639.
19. J. Wang, J. Long, Z. Liu, W. Wu, C. Hu, *Biosens. Bioelectron.*, 91 (2017) 53.
20. H. Karimi-Maleh, M. Alizadeh, Y. Orooji, F. Karimi, M. Baghayeri, J. Rouhi, S. Tajik, H. Beitollahi, S. Agarwal, V.K. Gupta, S. Rajendran, S. Rostamnia, L. Fu, F. Saberi-Movahed, S. Malekmohammadi, *Ind. Eng. Chem. Res.*, 60 (2021) 816.
21. H. Karimi-Maleh, A. Ayati, S. Ghanbari, Y. Orooji, B. Tanhaei, F. Karimi, M. Alizadeh, J. Rouhi, L. Fu, M. Sillanpää, *J. Mol. Liq.*, 329 (2021) 115062.
22. H. Karimi-Maleh, A. Ayati, R. Davoodi, B. Tanhaei, F. Karimi, S. Malekmohammadi, Y. Orooji, L. Fu, M. Sillanpää, *J. Clean. Prod.*, 291 (2021) 125880.
23. L. Gong, L. Feng, Y. Zheng, Y. Luo, D. Zhu, J. Chao, S. Su, L. Wang, *Biosensors*, 12 (2022) 87.
24. J. Wang, L. Sui, J. Huang, L. Miao, Y. Nie, K. Wang, Z. Yang, Q. Huang, X. Gong, Y. Nan, *Bioact. Mater.*, 6 (2021) 4209.
25. R.-I. Stefan-van Staden, R.-M. Ilie-Mihai, F. Pogacean, S.M. Pruneanu, *New J. Chem.*, 44 (2020) 20203.
26. C. Tan, X. Qian, Z. Guan, B. Yang, Y. Ge, F. Wang, J. Cai, *SpringerPlus*, 5 (2016) 467.
27. J.-Y. LIANG, T. Pei-Hong, L. Jian-Ping, *Chin. J. Anal. Chem.*, 47 (2019) 1283.
28. G. Ibáñez-Redín, R.H.M. Furuta, D. Wilson, F.M. Shimizu, E.M. Materon, L.M.R.B. Arantes, M.E. Melendez, A.L. Carvalho, R.M. Reis, M.N. Chaur, D. Gonçalves, O.N. Oliveira Jr, *Mater. Sci. Eng. C*, 99 (2019) 1502.
29. M. Mic, C. Varodi, F. Pogacean, C. Socaci, M. Coros, R.-I. Stefan-van Staden, S. Pruneanu, *Chemosensors*, 8 (2020) 112.
30. Y. Tian, X. Li, F. Wang, C. Gu, Z. Zhao, H. Si, T. Jiang, *J. Hazard. Mater.*, 403 (2021) 124009.
31. J. Guo, J. Yu, X. Song, H. Mi, *Open Med.*, 12 (2017) 131
32. M. Naguib, M. Kurtoglu, V. Presser, J. Lu, J. Niu, M. Heon, L. Hultman, Y. Gogotsi, M.W. Barsoum, *Adv. Mater.*, 23 (2011) 4248.
33. Z. Huang, Z. Jiang, C. Zhao, W. Han, L. Lin, A. Liu, S. Weng, X. Lin, *Int. J. Nanomedicine*, 12 (2017) 3049.
34. C. Wei, J. Xiao, S. Liu, Z. Wang, L. Chen, W. Teng, *Anal. Lett.* (2021) 1.
35. R.-I. Stefan-van Staden, R.-M. Ilie-Mihai, S. Gurzu, *Anal. Lett.*, 53 (2020) 2545.
36. L. Liu, T. Li, S. Zhang, P. Song, B. Guo, Y. Zhao, H. Wu, *Angew. Chem. Int. Ed.*, 57 (2018) 11882
37. R.I. Stefan-van Staden, R.M. Ilie-Mihai, S. Gurzu, *Multidiscip. Cancer Investig.*, 4 (2020) 25.
38. N. Murugan, R. Jerome, M. Preethika, A. Sundaramurthy, A.K. Sundramoorthy, *J. Mater. Sci. Technol.*, 72 (2021) 122.
39. U. Amara, M.T. Mehran, B. Sarfaraz, K. Mahmood, A. Hayat, M. Nasir, S. Riaz, M.H. Nawaz, *Microchim. Acta*, 188 (2021) 1.

40. M. Wu, Q. Zhang, Y. Fang, C. Deng, F. Zhou, Y. Zhang, X. Wang, Y. Tang, Y. Wang, *J. Colloid Interface Sci.*, 586 (2021) 20.
41. W. Xu, M. Sakran, J. Fei, X. Li, C. Weng, W. Yang, G. Zhu, W. Zhu, X. Zhou, *ACS Biomater. Sci. Eng.*, 7 (2021) 2767.
42. D. Cheng, P. Li, X. Zhu, M. Liu, Y. Zhang, Y. Liu, *Chin. J. Chem.*, 39 (2021) 2181.
43. M. Chen, H. Yang, Z. Song, Y. Gu, Y. Zheng, J. Zhu, A. Wang, L. Fu, *Phyton-Int. Exp. Bot.*, 90 (2021) 1507.
44. A. Rhouati, M. Berkani, Y. Vasseghian, N. Golzadeh, *Chemosphere* (2021) 132921.
45. M. Sajid, *Anal. Chim. Acta*, 1143 (2021) 267.
46. L. Fu, X. Zhang, S. Ding, F. Chen, Y. Lv, H. Zhang, S. Zhao, *Curr. Pharm. Anal.*, 18 (2022) 4.
47. L. Kashefi-Kheyrabadi, A. Koyappayil, T. Kim, Y.-P. Cheon, M.-H. Lee, *Bioelectrochemistry*, 137 (2021) 107674.
48. C. Liu, W. Yang, X. Min, D. Zhang, X. Fu, S. Ding, W. Xu, *Sens. Actuators B Chem.*, 334 (2021) 129585.
49. R.D. Nagarajan, A. Sundaramurthy, A.K. Sundramoorthy, *Chemosphere*, 286 (2022) 131478.
50. Z. Jiang, C. Zhao, L. Lin, S. Weng, Q. Liu, X. Lin, *Anal. Methods*, 7 (2015) 4508.
51. G. Ibáñez-Redín, E.M. Materon, R.H. Furuta, D. Wilson, G.F. do Nascimento, M.E. Melendez, A.L. Carvalho, R.M. Reis, O.N. Oliveira, D. Gonçalves, *Microchim. Acta*, 187 (2020) 417.